# Signaling to the Nucleus by an L-type Calcium Channel–Calmodulin Complex Through the MAP Kinase Pathway

**Ricardo E. Dolmetsch, Urvi Pajvani, Katherine Fife, James M. Spotts, Michael E. Greenberg***

Increases in the intracellular concentration of calcium ($[Ca^{2+}]_i$) activate various signaling pathways that lead to the expression of genes that are essential for dendritic development, neuronal survival, and synaptic plasticity. The mode of $Ca^{2+}$ entry into a neuron plays a key role in determining which signaling pathways are activated and thus specifies the cellular response to $Ca^{2+}$. $Ca^{2+}$ influx through L-type voltage-activated channels (LTCs) is particularly effective at activating transcription factors such as CREB and MEF-2. We developed a functional knock-in technique to investigate the features of LTCs that specifically couple them to the signaling pathways that regulate gene expression. We found that an isoleucine-glutamine ("IQ") motif in the carboxyl terminus of the LTC that binds $Ca^{2+}$-calmodulin (CaM) is critical for conveying the $Ca^{2+}$ signal to the nucleus. $Ca^{2+}$-CaM binding to the LTC was necessary for activation of the Ras/mitogen-activated protein kinase (MAPK) pathway, which conveys local $Ca^{2+}$ signals from the mouth of the LTC to the nucleus. CaM functions as a local $Ca^{2+}$ sensor at the mouth of the LTC that activates the MAPK pathway and leads to the stimulation of genes that are essential for neuronal survival and plasticity.

Voltage-gated $Ca^{2+}$ channels have a central role in neuronal function and are essential for converting electrical activity into biochemical events (*1*). Neurons express at least nine types of voltage-gated $Ca^{2+}$ channels that are specialized for different functions (*2*). Activation of the L-type $Ca^{2+}$ channel (LTC) specifically increases the expression of a group of $Ca^{2+}$-regulated genes, including those encoding c-Fos, brain-derived neurotrophic factor (BDNF), and Bcl-2, that are important for neuronal survival, learning, and other adaptive responses in the nervous system (*3*). The features of the LTC that specify its functions are not known, but one possibility is that $Ca^{2+}$-binding proteins bound to the channel sense the local $Ca^{2+}$ concentration and selectively activate signaling pathways when the channel opens. To test this idea, we developed a strategy to introduce exogenous LTCs into primary neurons and to examine their ability to activate nuclear signaling pathways. This approach has allowed us to separate the $Ca^{2+}$-conducting properties of the LTC from its signaling properties and has provided insight into the mechanism by which voltage-gated channels regulate gene expression.

**L-type calcium channels selectively signal to the nucleus.** We characterized the signaling properties of the endogenous LTC by monitoring the activation of the cyclic adenosine monophosphate (cAMP) response element binding protein (CREB) in cortical neurons (*4*). CREB drives the expression of a number of genes that regulate neuronal survival and plasticity (*5*). CREB is activated by phosphorylation of $Ser^{133}$, which allows recruitment of CREB binding protein (CBP) and initiation of transcription (*6*). After membrane depolarization, activation of CREB-dependent transcription depends critically on LTCs (*7*, *8*). Membrane depolarization of neurons to −30 mV leads to a sustained increase in CREB phosphorylation that is eliminated by dihydropyridine (DHP) LTC blockers, but is only slightly sensitive to blockers of *N*-methyl-D-aspartate (NMDA) receptors and is completely insensitive to blockers of other voltage-gated calcium channels (Fig. 1A) (*9*). A detailed time course of CREB phosphorylation in membrane-depolarized neurons, with an antibody that recognizes CREB phosphorylated at $Ser^{133}$ (*10*), revealed that CREB was phosphorylated after 1 min and remained phosphorylated for at least 40 min after the initial stimulus (Fig. 1B). However, in the presence of DHPs, CREB $Ser^{133}$ phosphorylation was transient and returned to resting levels after 20 min (Fig. 1C). This suggests that at early times CREB $Ser^{133}$ phosphorylation occurs independently of $Ca^{2+}$ influx through LTCs, but that sustained CREB $Ser^{133}$ phosphorylation depends on LTC activation. DHPs completely eliminate activation of a CREB-dependent reporter gene, suggesting that prolonged CREB $Ser^{133}$ phosphorylation is required for transcription (*11*).

To determine whether the unique ability of LTCs to produce sustained CREB $Ser^{133}$ phosphorylation arises because LTCs elevate the intracellular concentration of calcium ($[Ca^{2+}]_i$) to a greater extent than other channels, we measured $[Ca^{2+}]_i$ with fura-2 and digital $Ca^{2+}$ imaging (*12*). Membrane depolarization triggers a transient increase in $[Ca^{2+}]_i$ that is followed by a sustained plateau. We found that at 37°C in 2 mM extracellular $Ca^{2+}$, LTC blockers reduce the $[Ca^{2+}]_i$ during the plateau phase of the response by 15 to 20%, in agreement with electrophysiological findings in cultured neurons (Fig. 1D) (*13*). N- and P/Q-type channel blockers (ω-Conotoxin GVIA and ω-Agatoxin IVA) or NMDA receptor blockers (D,L,-2-amino-5-phosphonovaleric acid, D-APV) also reduced the plateau $[Ca^{2+}]_i$ by 15 to 20%. This suggests that N- and P/Q-type channels, NMDA receptors, and LTCs each contribute to the sustained $[Ca^{2+}]_i$ elevation in the cytoplasm and nucleus to a similar extent. About a third of the $[Ca^{2+}]_i$ rise was not blocked by a mixture of channel blockers (ω-Conotoxin GVIA, ω-Agatoxin IVA, nimodipine, and D-APV, which block N-, P/Q-, and L-type voltage-gated channels and NMDA receptors, respectively), suggesting that a portion of the $[Ca^{2+}]_i$ rise may be due to influx through R-type channels that are insensitive to these blockers. Even though the global increase in $[Ca^{2+}]_i$ is about the same in the presence of LTC blockers as in the presence of NMDA receptor and N- and P/Q-type channel blockers, LTC blockers completely eliminate CREB-dependent reporter gene expression, whereas N- and P/Q-type channel blockers do not. This is consistent with the idea that CREB-dependent transcription is most effectively activated by $Ca^{2+}$ influx through LTCs.

We further tested the idea that $Ca^{2+}$ influx through LTCs signals preferentially to CREB relative to $Ca^{2+}$ influx through other voltage-gated channels. CREB activation was measured in neurons that were depolarized in the presence of LTC or non-LTC blockers and various concentrations of extracellular $Ca^{2+}$. By changing the $Ca^{2+}$ gradient across the membrane, it was possible to control the $Ca^{2+}$ influx through LTCs or non-LTCs (R-, N-, and P/Q-type channels). This experiment allowed us to determine if prolonged CREB $Ser^{133}$ phosphorylation and activation of CREB-dependent transcription was a function of the $Ca^{2+}$ elevation in the cell body and in the nucleus, or whether it depended on

Division of Neuroscience, Children's Hospital and Department of Neurobiology, Harvard Medical School, Enders Pediatric Research Laboratories, Room 260, 300 Longwood Avenue, Boston, MA 02115, USA.

*To whom correspondence should be addressed. E-mail: michael.greenberg@tch.harvard.edu

the activation of specific types of channels. After 30 min of membrane depolarization in the presence of non-LTC blockers (ω-Conotoxin GVIA, ω-Agatoxin IVA), increases in the extracellular $Ca^{2+}$ concentration led to corresponding increases in CREB $Ser^{133}$ phosphorylation (Fig. 1E) and CREB-dependent transcription (Fig. 1G). In contrast, in the presence of the LTC blocker nimodipine these same concentrations of extracellular $Ca^{2+}$ failed to induce CREB $Ser^{133}$ phosphorylation (Fig. 1F) and activation of a CREB-dependent reporter gene (Fig. 1G). A plot of CREB reporter gene activity as a function of $[Ca^{2+}]_i$ either in the presence of LTC or non-LTC blockers revealed that even at high $[Ca^{2+}]_i$, the $Ca^{2+}$ that entered through channels other than LTCs did not activate CREB (Fig. 1G).

**A functional knock-in of the L-type channel.** To determine what features of the LTCs are responsible for their selective ability to activate CREB, we transfected neurons with recombinant LTCs that could be distinguished from the endogenous channels. To do this, we constructed a mutant LTC that is insensitive to DHPs and expressed this channel in primary cultured neurons. We then treated the neurons with DHPs to block the endogenous channels and examined the ability of the transfected channels to activate signal transduction pathways in response to membrane depolarization. By introducing deletions or substitutions within the cytoplasmic domains of the DHP-resistant channels, we investigated whether these domains were critical for LTC signaling to the nucleus.

Voltage-gated $Ca^{2+}$ channels are oligomers composed of a pore-forming α1 subunit and β, α2δ, and in some cases γ subunits. Channels containing the α1C (CaV1.2) subunit form a major class of neuronal LTCs (*14*). We constructed an α1C subunit containing a threonine to tyrosine point mutation at position 1039 and an epitope tag at the $NH_2$-terminus [DHP-LTC; (*15*)]. This mutant subunit is at least 100 times less sensitive to DHP blockers of LTCs than are wild-type channels (*16*). We transfected cortical neurons with plasmids (*17*) encoding the mutant α1C subunit, β1b, and α2δ subunits and used antibodies against the epitope tag to verify the localization of the DHP-LTC (Fig. 2A). The DHP-LTC was uniformly expressed in the cell body and dendrites of the neurons in a pattern similar to that reported for the endogenous L-type channel (*18*). To determine whether the DHP-LTC was inserted into the plasma membrane and could permit $Ca^{2+}$ influx, we measured $[Ca^{2+}]_i$ in DHP-LTC–transfected neurons after membrane depolarization with 60 mM KCl in the presence of nimodipine, APV, ω-Conotoxin MVIIC, and ω-Agatoxin-IVA (Fig. 2B). This cocktail of blockers inhibited most of the endogenous $[Ca^{2+}]_i$ rise at 25°C but did not block $Ca^{2+}$ influx through the DHP-LTC. Neurons transfected with DHP-LTCs displayed an average $[Ca^{2+}]_i$ rise that was 318 ± 57 nM (mean ± SEM, $n$ = 64) higher than that detected in either untransfected neurons in the same field or cells transfected with a wild-type (DHP-sensitive) channel (Fig. 2C). These results indicate that the DHP-LTC is expressed in primary cortical neurons, is inserted in the plasma membrane, and can elevate $[Ca^{2+}]_i$ even in the presence of LTC blockers.

We then investigated whether the DHP-LTC can activate CREB when transfected into neurons. Neurons were transfected with the DHP-LTC, depolarized in the presence of nimodipine and APV, and stained with antibodies that specifically bind CREB phosphorylated on $Ser^{133}$ (*19*). Membrane depolarization of DHP-LTC–transfected and nimodipine-treated cells induced sustained phosphorylation of CREB $Ser^{133}$ (Fig. 2D), suggesting that the transfected channels are coupled to the signaling machinery that leads to long-lasting CREB phosphorylation (Fig. 2D). In contrast, when neurons transfected with wild-type LTCs were depolarized in the presence of nimodipine, CREB $Ser^{133}$ phosphorylation was not observed (Fig. 2E). Because phosphorylation of CREB at $Ser^{133}$ is necessary but not always sufficient for CREB-dependent transcription (*20*), we also determined if DHP-LTC activation could trigger CREB-dependent transcription. Membrane depolarization in the presence of nimodipine increased CREB reporter-gene activation in neurons expressing the DHP-LTC, but not in neurons transfected with the wild-type LTC. DHP-LTC–induced expression of the CREB reporter gene was blocked by diltiazem, a non-DHP blocker of LTCs, indicating that reporter gene activation was mediated by $Ca^{2+}$ influx through the DHP-LTC (Fig. 2G). Thus, the transfected DHP-LTCs are effectively coupled to signaling pathways in neurons and can trigger CREB-dependent transcription upon membrane depolarization.

**The IQ domain is required for signaling to the nucleus.** To investigate whether cytoplasmic regions of the LTC are necessary for signaling to CREB, we introduced mutations into cytoplasmic domains of the DHP-LTC and assessed the effect of these mutations on the ability of the channel to convey

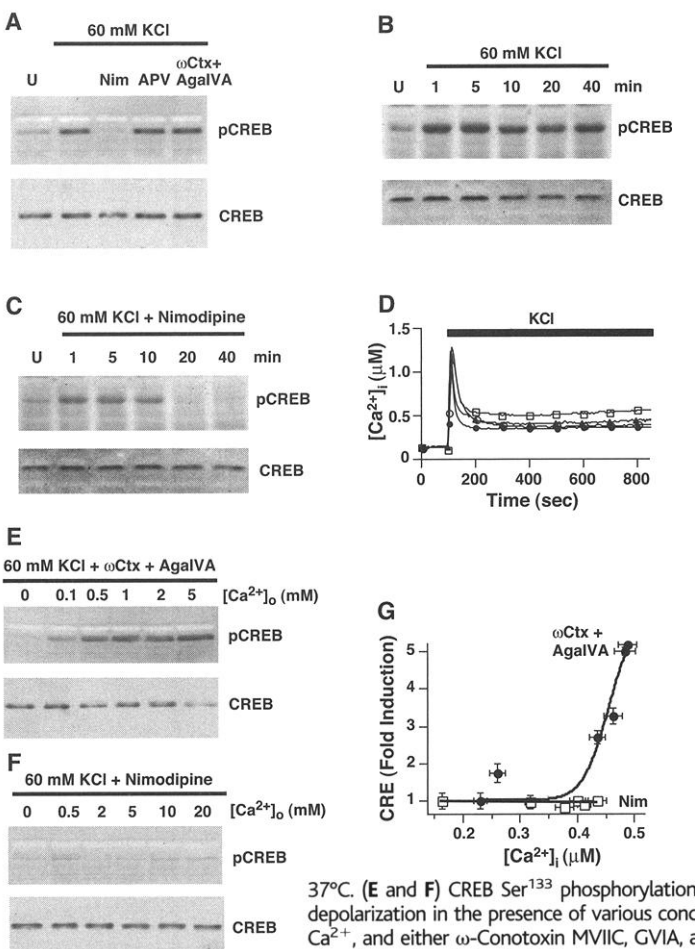


**Fig. 1.** $Ca^{2+}$ influx through LTCs is linked to sustained CREB $Ser^{133}$ phosphorylation and transcriptional activation. (**A**) Western blot of neurons depolarized with 60 mM KCl for 40 min and probed with antibodies to phospho-CREB $Ser^{133}$. CREB $Ser^{133}$ phosphorylation is blocked by nimodipine, but is insensitive to APV or a mixture of ω-Conotoxin MVIIC, GVIA, and ω-Agatoxin IVA. Membranes were stripped and reprobed with anti-CREB. (**B** and **C**) The time course of CREB $Ser^{133}$ phosphorylation in the absence (B) or presence (C) of nimodipine. (**D**) Average $[Ca^{2+}]_i$ responses of neurons loaded with Fura-2 and depolarized with 60 mM KCl alone (□) or with 60 mM KCl and 5 μM Nimodipine (▲), 100 μM APV (○), or 1 μM ω-Conotoxin MVIIC, GVIA, and ω-Agatoxin IVA (●; $n$ > 250 for all conditions) at 37°C. (**E** and **F**) CREB $Ser^{133}$ phosphorylation 40 min after membrane depolarization in the presence of various concentrations of extracellular $Ca^{2+}$, and either ω-Conotoxin MVIIC, GVIA, and ω-Agatoxin IVA (E) or nimodipine (F). Note that the extracellular $Ca^{2+}$ concentrations are higher in (F) than in (E). (**G**) $[Ca^{2+}]_i$ dependence of activation of a CRE-luciferase gene in neurons stimulated as in (E) (●) or (F) (□). Average $[Ca^{2+}]_i$ corresponds to the plateau phase of the response. Error bars are SEMs ($n$ = 5).

the $Ca^{2+}$ signal to CREB. We focused on the COOH-terminus of the channel that binds the $Ca^{2+}$-binding protein calmodulin (CaM) (Fig. 3A) (*21–23*). Deletion of the full COOH-terminus containing the IQ domain (Trunc-IQ) completely abolished signaling to CREB (Fig. 3, B and C), but also eliminated the channel's ability to carry $Ca^{2+}$ (Fig. 3E). However, an LTC truncation mutant that deleted the COOH-terminus immediately downstream of the IQ motif (Trunc+IQ) was expressed in normal amounts (Fig. 3D) and elevated $[Ca^{2+}]_i$ normally upon membrane depolarization (Fig. 3E), but conferred diminished activation of a CREB-dependent reporter gene (Fig. 3C). In neurons expressing this mutant LTC, CREB was phosphorylated at $Ser^{133}$ at early time points (1 and 5 min), but phosphorylation at this site was significantly reduced at 30 min. This suggests that an LTC with a truncated COOH-terminus is defective in long-term activation of CREB (Fig. 3B). These results indicate that the LTC is not merely a conduit for $Ca^{2+}$, but that it can directly activate signaling pathways that lead to prolonged CREB phosphorylation and transcriptional activation.

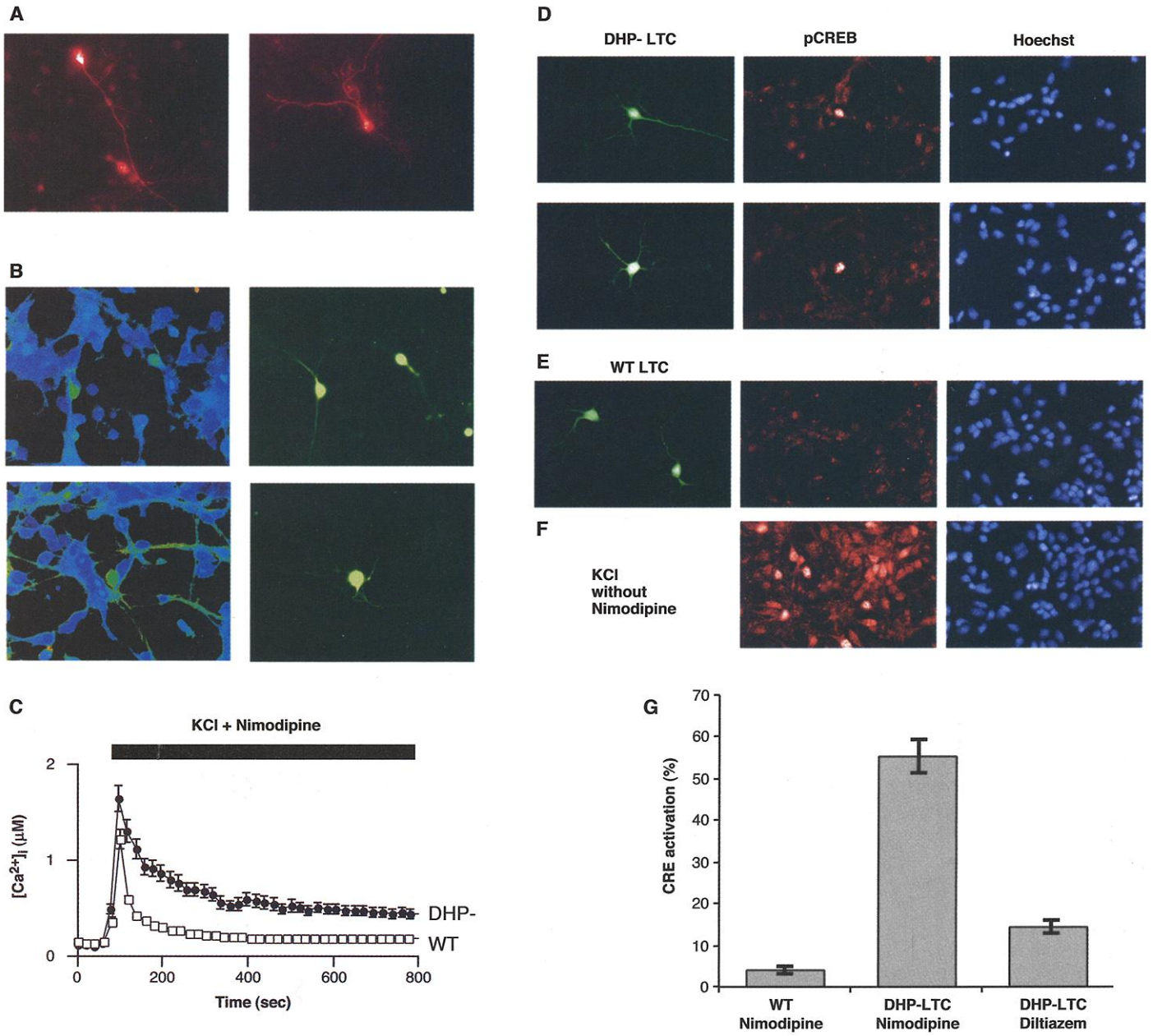


**Fig. 2.** The DHP-LTC is expressed in neurons, elevates $[Ca^{2+}]_i$, and activates CREB **(A)** Immunostaining of cortical neurons transfected with epitope-tagged DHP-LTCs. **(B)** Pseudocolor images of neurons loaded with Fura-2 and stimulated with KCl in the presence of a mixture of nimodipine, APV, ω-Conotoxins, and ω-Agatoxin IVA (left) taken 250 s after stimulation. Elevated $[Ca^{2+}]_i$ is shown in green and resting $[Ca^{2+}]_i$ is shown in blue. (Right) Neurons transfected with DHP-LTCs and GFP. **(C)** Average $[Ca^{2+}]_i$ response of a population of neurons stimulated as in (B) and transfected with DHP- LTCs (●, $n$ = 65) or with wild-type DHP-sensitive LTCs (□, $n$ = 58). **(D)** Neurons transfected with DHP-LTC and GFP (left) depolarized in the presence of nimodipine for 40 min and stained with anti–phospho-CREB $Ser^{133}$ (center) and the nuclear stain Hoechst 33342 (right). **(E)** Neurons transfected with a wild-type LTC and treated as in (D). **(F)** Untransfected neurons stimulated with KCl in the absence of nimodipine, stained with anti–pCREB $Ser^{133}$ (center) and Hoechst 33342 (right). **(G)** Activation of a CREB-dependent reporter gene (CRE-luciferase) in neurons cotransfected with either wild-type LTCs or DHP-LTCs and CRE-luciferase. Neurons were membrane depolarized with 60 mM KCl in the presence of 5 μM nimodipine or 100 μM diltiazem and analyzed for luciferase expression after 6 hours. CRE-luciferase activation is shown as a percentage of the maximal activation of the CRE-luciferase gene in the transfected cells in the absence of channel blockers.

The Trunc+IQ mutant channel could be defective in activating CREB either because it eliminates binding of signaling proteins to the COOH-terminus or because it disrupts the binding of CaM to the IQ motif itself. To investigate the first possibility, we generated two additional channel mutants with truncations further downstream of the IQ motif and tested their ability to signal to CREB. These truncated channels were as effective as the DHP-LTC in conferring CREB-dependent reporter gene activation (*36*), suggesting that the COOH-terminal half of the COOH-terminus is not required for LTC signaling to CREB. To test whether CaM binding to the IQ motif is required for signaling to CREB, we generated point mutants that specifically disrupted CaM binding to this region (*24*). DHP-LTCs bearing point mutations of isoleucine 1627 in the IQ motif to alanine (IA), cysteine (IC), glutamate (IE), or threonine (IT) were transfected into neurons along with a CREB-dependent reporter gene. The IQ mutant channels were substantially impaired in their ability to lead to CREB-dependent transcription (Fig. 4A) and prolonged CREB phosphorylation in depolarized neurons, although they were expressed at levels similar to those of the DHP-LTC (Fig. 4B). To investigate whether the defect in the ability of the IQ mutant DHP-LTC to signal to CREB was due to a failure to elevate $[Ca^{2+}]_i$ upon membrane depolarization, we measured depolarization-induced changes in $[Ca^{2+}]_i$ in neurons transfected with the IQ mutant DHP-LTCs (Fig. 4, C to E). With the exception of the IE mutant, all the IQ mutants generated a sustained $[Ca^{2+}]_i$ rise that was indistinguishable from that of the DHP-LTC with an intact IQ domain. The IE mutant generated a transient $[Ca^{2+}]_i$ rise that subsequently decayed rapidly to baseline (Fig. 4E). This may account for the lack of CREB activation in this mutant because sustained LTC activity is necessary for prolonged CREB phosphorylation. However, the decreased ability of the IA, IC, and IT mutants to activate CREB does not arise from premature channel inactivation, but instead implies an important role of CaM binding to the LTC for signaling to CREB.

LTCs with point mutations in the IQ domain are defective in $Ca^{2+}$-dependent channel inactivation (*22*). $Ca^{2+}$-dependent inactivation of the LTC could be required for signaling to CREB either by limiting the duration of the $[Ca^{2+}]_I$ rise or by directly coupling changes in the conformation of the channel to activation of signaling pathways. To determine whether $Ca^{2+}$-dependent inactivation is required for LTC signaling to CREB, we introduced two point mutations in the EF hand region of the LTC to generate two channels in which the VVTL motif at position 1548 is substituted with either VYTL or MYTL. The VYTL and MYTL channels are defective in $Ca^{2+}$-dependent inactivation (*25*), but contain an intact IQ motif and thus bind $Ca^{2+}$-CaM. Neurons expressing these mutant EF hand DHP-LTCs showed slightly larger increases in $[Ca^{2+}]_i$ than cells expressing the DHP-LTC channel, reflecting the lack of $Ca^{2+}$-dependent inactivation in the mutant proteins. The mutant EF hand DHP-LTCs fully induced CREB phosphorylation and activation of a CREB-dependent reporter gene (Fig. 4F), suggesting that LTC inactivation is not required for signaling to CREB. We conclude that the defects in signaling of the LTCs in which the IQ region is mutated are due to an additional requirement of CaM binding to the LTC for conveying the $Ca^{2+}$ signal to the nucleus.

**Calmodulin bound to L-type channels signals to the nucleus.** To obtain further support for the hypothesis that CaM binding to the LTC is important for signaling to the nucleus, we blocked CaM binding to the IQ motif of the wild-type LTC and assessed LTC activation of CREB-dependent transcription. In addition to binding to the IQ motif in a $Ca^{2+}$-dependent manner, CaM also binds the LTC at a second site in a $Ca^{2+}$-independent manner (*21*, *24*). Previous studies suggested that CaM is constitutively anchored to the LTC through the second site and then binds the IQ motif upon channel activation. One prediction of this model of CaM binding to the LTC is that overexpression of a mutant CaM that is defective in $Ca^{2+}$ binding, but that preserves the ability to bind to the LTC through the second site, should displace the endogenous CaM bound to the LTC. Upon LTC activation, the mutant CaM would not bind $Ca^{2+}$ and therefore could not interact with the IQ domain of the LTC. Thus, overexpression of the mutant CaMs would be predicted to block signaling to the nucleus by the IQ domain of the LTC.

We investigated the effect on CREB activation of overexpressing mutant CaMs that are defective in $Ca^{2+}$ binding (*26*). Transfection of neurons with a CaM mutant that lacks three of the four $Ca^{2+}$ binding sites inhibited depolarization-induced activation of a CREB-dependent gene by 54 ± 3% (SEM, $n = 4$). A CaM mutant that lacks all four $Ca^{2+}$ binding sites resulted in 62 ± 1% (SEM, $n = 4$) inhibition relative to that measured with a vector control (Fig. 4G). Overexpression of wild-type CaM augmented CREB reporter-gene activation by 70%, confirming that CaM plays an important role in signaling to CREB. These results are consistent with the idea that CaM binding to the IQ motif of the LTC is important for signaling to CREB. It should be noted that the mutant CaMs mimic $Ca^{2+}$-free CaM and thus do not bind to CaM targets that are activated by

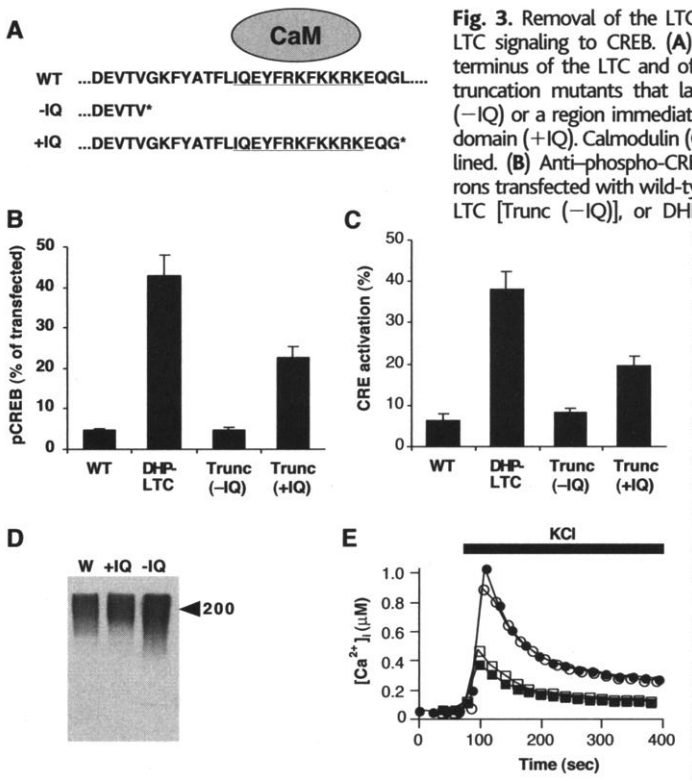


**Fig. 3.** Removal of the LTC COOH-terminus inhibits LTC signaling to CREB. **(A)** Diagram of the COOH-terminus of the LTC and of the LTC COOH-terminal truncation mutants that lack either the IQ domain (−IQ) or a region immediately downstream of the IQ domain (+IQ). Calmodulin (CaM) binding site is underlined. **(B)** Anti–phospho-CREB $Ser^{133}$ staining in neurons transfected with wild-type LTCs, DHP-LTCs, DHP-LTC [Trunc (−IQ)], or DHP-LTC [Trunc (+IQ)] and stimulated with KCl and nimodipine. The graph shows the percentage of neurons that are both transfected with the DHP-LTCs and positive for phospho-CREB $Ser^{133}$ ($n = 4$; ± SEM). **(C)** Activation of a CREB-dependent reporter gene in neurons transfected with the DHP-LTCs and stimulated as in (B). The graph shows CREB-dependent reporter gene activation as a percentage of the maximum activation observed in sister cultures stimulated in the absence of nimodipine ($n = 4$; ± SEM). **(D)** Western blot of human embryonic kidney (HEK) cells expressing either DHP-LTC, DHP-LTC -IQ, or DHP-LTC +IQ channels with anti-α1C shows that they are all expressed at approximately equal levels. **(E)** Average $[Ca^{2+}]_i$ measurements in membrane-depolarized neurons expressing the DHP-LTC +IQ (●; $n = 30$); the DHP-LTC (○; $n = 64$); the DHP-LTC -IQ channel (■; $n = 36$); or the wild-type LTC (□; $n = 67$) in the presence of nimodipine, APV, ω-Conotoxins, and ω-Agatoxin IVA.

$Ca^{2+}$-CaM (*27*). Therefore, the mutant CaMs should not inhibit activation of $Ca^{2+}$-CaM–activated proteins like the CaM kinases that are known to signal to CREB. However, the CaM mutants could prevent proteins, other than the LTC, that bind CaM in a $Ca^{2+}$-independent manner from signaling to the nucleus.

In addition to CREB, a number of other transcription factors have been shown to be dependent on $Ca^{2+}$ fluxes through the LTC. One such factor is MEF-2, a MADS domain transcription factor that mediates muscle differentiation and neuronal survival (*28*, *29*). To determine whether $Ca^{2+}$ signaling to MEF-2 is also dependent on CaM binding to the LTC, we transfected neurons with the IQ mutant DHP-LTCs and tested their ability to activate a MEF-2–dependent reporter gene upon membrane depolarization in the presence of DHPs (Fig. 5A). All of the IQ mutants and the COOH-terminal truncation mutant were deficient in their ability to activate MEF-2–dependent transcription. We also measured activation of a MEF-2–dependent reporter gene in neurons transfected with mutant CaMs that do not bind $Ca^{2+}$ (Fig. 5B). We found a reproducible suppression of MEF-2–dependent transcription by the mutant CaMs, suggesting that CaM binding to the IQ motif of the LTC activates a signaling pathway that participates in the activation of both MEF-2 and CREB.

**Calmodulin binding to L-type channels activates CREB by way of the MAPK pathway.** CaM binding to the IQ motif of the LTC must activate key signal transduction pathways that convey the $Ca^{2+}$ signal to the nucleus. Several different $Ca^{2+}$-regulated signaling pathways have been identified that trigger CREB and MEF-2 activation. These include the mitogen-activated protein kinase (MAPK/Erk) pathway (*30*, *31*) and the calmodulin-activated kinase IV (CaMK IV) pathway (*11*). We assessed the role of the Ras-MAPK pathway in LTC signaling to the nucleus because this pathway appears to account for the late phase of CREB phosphorylation (*32*) and because MAPK inhibitors effectively inhibit $Ca^{2+}$-dependent activation of MEF-2 in neurons (*33*). In addition, it has been shown that CaMK-II and -IV can be activated in isolated nuclei independently of LTCs, suggesting that they respond to bulk increases in $[Ca^{2+}]_i$ levels rather than to the selective influx of $Ca^{2+}$ through LTCs (*34*).

We depolarized neurons in the presence or absence of nimodipine and either immunoblotted neuronal lysates (Fig 6, A and B) or immunostained neurons (Fig. 6C) with an antibody that specifically detects phosphorylated and activated forms of Erk-1 and Erk-2. Erk activation occurred within 1 min of membrane depolarization, and the kinase remained active for at least 40 min (Fig. 6A). As with CREB, the early phase of Erk activation (1 and 5 min) was not blocked by DHPs, whereas Erk activation at later time points (10, 20, and 40 min) was DHP-sensitive (Fig. 6B). This indicates that the prolonged activation of the Erks requires $Ca^{2+}$ influx through the LTC and raises the possibility that Erk activation is required for the late phase of CREB phosphorylation.

To determine whether $Ca^{2+}$ influx through the LTC is sufficient for sustained activation of Erk, we transfected neurons

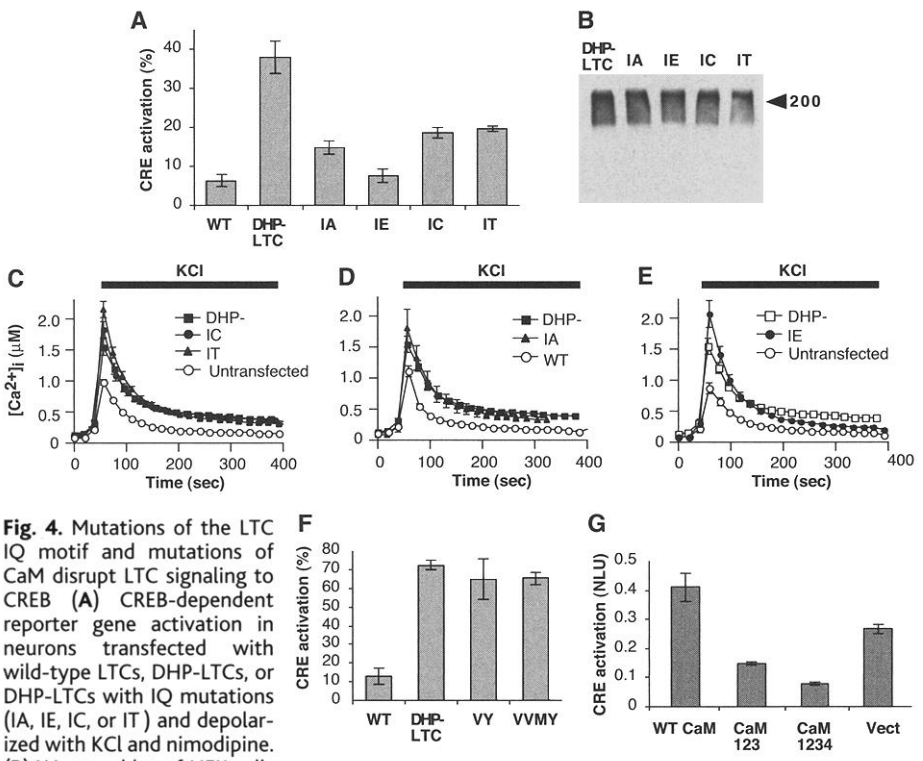


**Fig. 4.** Mutations of the LTC IQ motif and mutations of CaM disrupt LTC signaling to CREB (**A**) CREB-dependent reporter gene activation in neurons transfected with wild-type LTCs, DHP-LTCs, or DHP-LTCs with IQ mutations (IA, IE, IC, or IT) and depolarized with KCl and nimodipine. (**B**) Western blot of HEK cells expressing DHP-LTCs and IQ mutant channels. (**C** to **E**) $[Ca^{2+}]_i$ elevation in neurons transfected with DHP-LTCs, wild-type LTCs, or DHP-LTC IQ mutants. Neurons were depolarized with KCl in the presence of nimodipine, APV, ω-Conotoxins, and ω-Agatoxin IVA 35 s after the start of the recording. All the IQ mutant DHP-LTCs, with the exception of the IE mutant (E), elevate $[Ca^{2+}]_i$ to a greater extent than the endogenous channels (untransfected) or than wild-type LTCs and to the same extent as the DHP-LTC ($n > 35$; ±SEM). (**F**) CREB-dependent gene activation in neurons transfected with wild-type LTCs, DHP-LTCs, or DHP-LTCs EF hand mutants that lack $Ca^{2+}$-dependent inactivation (VY and VVMY; $n = 4$; ±SEM). (**G**) CREB-dependent gene activation in neurons transfected with wild-type CaM (WT), two CaM mutants (123 and 1234) that lack $Ca^{2+}$ binding, or a vector control along with a CRE-luciferase reporter gene ($n = 4$; ±SEM). CRE-luciferase values were normalized to the activity of a constitutively active renilla luciferase vector to control for transfection efficiency. Normalized luciferase values are shown.

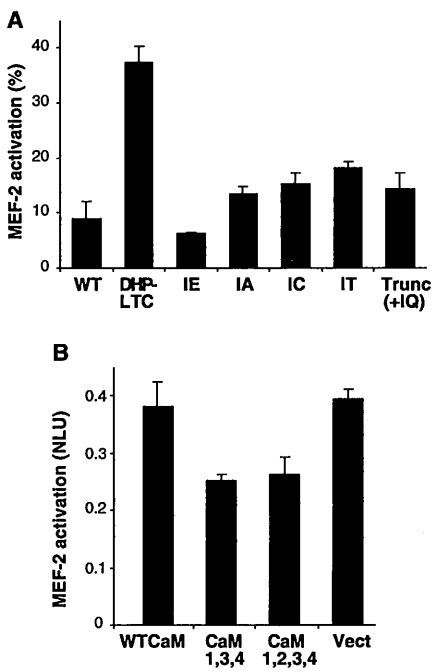


**Fig. 5.** Mutations of the LTC IQ motif and mutations of CaM disrupt LTC signaling to MEF-2. (**A**) MEF-2 transcriptional activation in neurons transfected with the LTC, DHP-LTC, or IQ mutant DHP-LTC and a MEF-2–dependent reporter gene (MRE luciferase; $n = 8$). Neurons were membrane-depolarized in the presence of nimodipine and analyzed after 6 hours. (**B**) MEF-2 reporter gene activation in neurons transfected with wild-type CaM, CaM with mutations in three or four of the aspartates that are critical for $Ca^{2+}$ binding, or with a vector control and an MEF-2–dependent reporter gene. Normalized luciferase units (NLU) are shown ($n = 4$).

with DHP-LTCs, depolarized the neurons in the presence of DHPs, and then stained the neurons with antibodies to activated Erk. We found that Erk-1 and Erk-2 were activated for at least 20 min after membrane depolarization in the presence of DHPs in cells transfected with DHP-LTCs, but not in cells transfected with wild-type channels (Fig. 6D). This suggests that $Ca^{2+}$ influx through the LTC is sufficient for sustained Erk activation. All the DHP-LTC IQ mutants were deficient in activation of Erk-1 and Erk-2, implying that CaM binding to the IQ motif of the LTC is necessary for prolonged activation of Erk in neurons (Fig. 6E). We also examined whether MAPK activation was inhibited by the mutant CaMs that are deficient in $Ca^{2+}$ binding. The mutant CaMs suppressed activation of Erk-1 and Erk-2 in neurons, suggesting that LTC induction of sustained MAPK activation also requires CaM binding to the IQ motif of the LTC (Fig. 6F). Taken together with the findings on LTC regulation of CREB- and MEF-2–dependent transcription, these results indicate that upon membrane depolarization, $Ca^{2+}$-dependent binding of CaM to the IQ motif of the LTC stimulates the MAPK pathway and leads to the activation of CREB and MEF-2

**Conclusions.** We have developed a general method for investigating which structural features of LTCs are required for signaling in neurons. The system involves making mutant channels that are resistant to pharmacological blockers, transfecting the mutant channels into neurons, and using the blockers to eliminate signaling by the endogenous channels. This allows signaling by the transfected channels to be studied in isolation. The approach can be used to examine the structural requirements for channel signaling in primary cells that express LTCs and allows rapid screening of channel mutants in cell culture before investigating their function in intact animals. A similar approach may also be useful for studying the function of other channels such as NMDA receptors, which interact with a diverse array of signaling proteins and for which highly specific blockers are available.

In this study, we have used the pharmacological knock-in strategy to investigate what regions of LTCs are necessary for signaling to CREB and MEF-2. Our results are consistent with a model in which $Ca^{2+}$ entering through LTCs binds CaM tethered to the channel, causing it to associate with the IQ motif of the LTC. Once associated with the IQ motif, CaM either triggers a conformational change in the LTC or directly binds to other signaling proteins that are associated with the cytoplasmic regions of the LTC. These changes activate MAPK cascades by mechanisms that remain to be clarified, and culminate in CREB and MEF-2 activation.

Two mechanisms for linking $[Ca^{2+}]_i$ elevations to the activation of CREB have been proposed. First, $Ca^{2+}$ itself may enter the nucleus and activate nuclear kinases that lead to CREB phosphorylation (*35*). Alternatively, $Ca^{2+}$ may act locally near the membrane to generate a second signal that leads to the activation of nuclear kinases (*8*). Our data indicate that both of these mechanisms may operate in neurons under different circumstances. When $Ca^{2+}$ is elevated above a threshold in the nucleus shortly after depolarization, it can activate nuclear CaM kinases and lead to activation of CREB; however, when $Ca^{2+}$ concentrations in the nucleus fall below a threshold, then the MAPK pathway that is activated close to the plasma membrane by $Ca^{2+}$ influx through LTCs appears to predominate.

The specificity of the LTC for signaling to the nucleus probably does not arise from its ability to bind CaM per se, but rather from the ability of the LTC to use CaM to activate other signaling molecules associated with the LTC. Our preliminary evidence suggests that scaffolding proteins bound to an LTC cytoplasmic domain may recruit Ras/MAPK activators, allowing CaM to activate them directly or indirectly through a conformational change in the channel. This suggests that the LTC acts like a receptor for $Ca^{2+}$ that is capable of recruiting signaling molecules and activating them in a $Ca^{2+}$-dependent manner.

The tethering of CaM to the LTC and the $Ca^{2+}$-dependent binding of CaM to an IQ domain as an initial step in the activation of signaling pathways may be a general feature of voltage-activated $Ca^{2+}$ channels. In addition to the LTC, several other voltage-gated $Ca^{2+}$ channels have IQ domains that are thought to bind CaM (*23*) and could participate in activating signaling proteins bound to intracellular domains of the channels. This mechanism may regulate a wide variety of $Ca^{2+}$-activated cellular processes, including

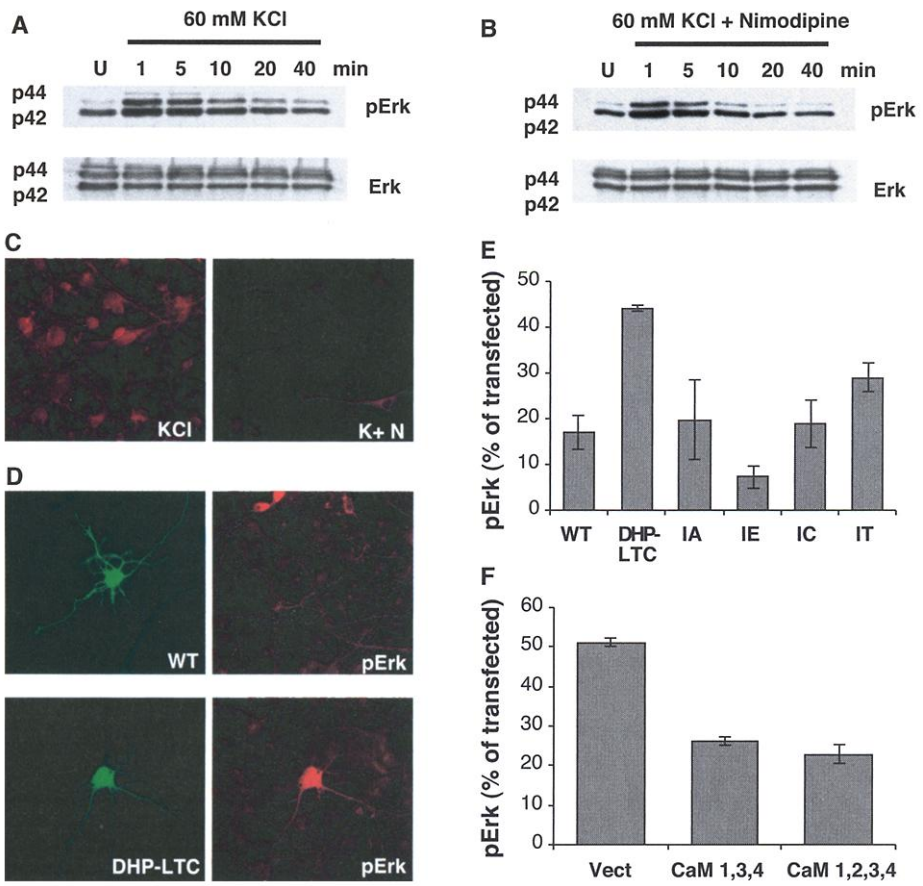


**Fig. 6.** CaM binding to the LTC IQ motif is required for sustained MAPK activation by LTCs. (**A** and **B**) $Ca^{2+}$ influx through LTCs results in sustained Erk phosphorylation. Western blot of the time course of p42 or p44 Erk $Thr^{202}/Tyr^{204}$ phosphorylation in cortical neurons depolarized with KCl in the absence (A) or presence (B) of nimodipine. Blots were stripped and reprobed with anti-p42/p44. (**C**) Neurons immunostained with anti–phospho-Erk 10 min after depolarization with KCl (left) or with KCl and nimodipine (right). (**D**) Neurons transfected with wild-type LTC or DHP-LTC and GFP were depolarized in the presence of nimodipine and stained with the anti–phospho-Erk. (**E**) Quantitation of anti–phospho-Erk staining in the nuclei of neurons transfected with LTCs, DHP-LTCs, or DHP-LTCs with mutations in the IQ domain and depolarized as in (D). The graph shows the percentage of transfected cells (GFP positive) that also have phospho-Erk–positive nuclei ($n = 4$) (**F**) Percentage of phospho-Erk–positive nuclei in neurons transfected with a vector control or with CaMs that are deficient in binding $Ca^{2+}$ ($n = 4$).

neurotransmitter release and cytoskeletal remodeling. Thus, CaM binding to $Ca^{2+}$ channels not only modulates channel activity but may also play a pivotal role in activating signaling cascades that regulate transcription and neuronal function.

**References and Notes**


1. M. J. Berridge, *Neuron* **21**, 13 (1998).
2. W. A. Catterall, *Annu. Rev. Cell Dev. Biol.* **16**, 521 (2000).
3. A. E. West *et al.*, *Proc. Natl. Acad. Sci. U.S.A.* **98**, 11024 (2001).
4. Cortical neurons were cultured from E17-E19 Long-Evans rats as described (37), plated at a density of $1 \times 10^6$ cells per well of a 12-well plate (Falcon), and maintained for 4 to 6 days in Basal Medium Eagle (Sigma) containing 5% fetal calf serum, penicillin, streptomycin, and 1% glucose. Cells were stimulated in Tyrodes solution containing 75 mM NaCl, 65 mM KCl, 2 mM $CaCl_2$, 1 mM $MgCl_2$, 25 mM Hepes, 10 mM glucose, and 0.1% bovine serum albumin. Where indicated, LTCs were blocked with 5 μM nimodipine and 100 μM diltiazem (racemic) (Sigma); P/Q- and N-type channels were blocked with 1 μM ω-Agatoxin IVA, 1 μM ω-Conotoxin GIVA, and 1 μM ω-Conotoxin MVIIC (Alomone Labs). Blockers were usually added 30 min before stimulation.
5. A. J. Shaywitz, M. E. Greenberg, *Annu. Rev. Biochem.* **68**, 821 (1999).
6. J. C. Chrivia *et al.*, *Nature* **365**, 855 (1993).
7. H. Bading, D. D. Ginty, M. E. Greenberg, *Science* **260**, 181 (1993).
8. K. Deisseroth, E. K. Heist, R. W. Tsien, *Nature* **392**, 198 (1998).
9. For Western blots, cells were lysed in boiling SDS lysis buffer, separated by SDS–polyacrylamide gel electrophoresis, and transferred onto polyvinylidene difluoride membranes before antibody staining. The following antibodies were purchased: anti–LTC α1C (Chemicon), anti–phospho-Erk $Thr^{202}/Tyr^{204}$ (Cell Signaling and Promega), anti-Erk1/2 (Upstate Biotechnology), and anti-Xpress (Invitrogen). The development of anti–phospho-CREB $Ser^{133}$ and anti-CREB antibodies has been described (*10*).
10. D. D. Ginty *et al.*, *Science* **260**, 238 (1993).
11. H. Bito, K. Deisseroth, R. W. Tsien, *Cell* **87**, 1203 (1996).
12. For $Ca^{2+}$ imaging experiments, neurons were loaded with 1 μM fura-2 for 20 min at 37°C in Tyrodes solution. Imaging was performed at 25° or 37°C, as indicated, on an inverted epifluorescence microscope (Nikon Eclipse) equipped with a xenon arc lamp, an excitation filter wheel, and a cooled charge-coupled device (CCD) camera. Open Lab software (Improvision) was used to collect and quantitate time-lapse excitation-ratio images. Ratio values were converted to $[Ca^{2+}]_i$ by using a standard curve of fura-2 ratio emission values as a function of $Ca^{2+}$, measured in a cuvette on the microscope stage with calibrated EGTA/$Ca^{2+}$ solutions (Molecular Probes).
13. A. Randall, R. W. Tsien, *J. Neurosci.* **15**, 2995 (1995).
14. T. P. Snutch, W. J. Tomlinson, J. P. Leonard, M. M. Gilbert, *Neuron* **7**, 45 (1991).
15. The coding sequence for α1C derived from mammalian brain (RBCII) was a gift of T. Snutch. It was subcloned into the Topo-adapted pcDNA-4 vector (Invitrogen). Site-directed mutagenesis to generate the DHP-LTC, IQ, and EF mutants was performed with the QuickChange system (Stratagene) and was always followed by complete sequencing of the resulting channel. The EF hand mutations consisted of changing the VVTL motif at position 1548 with VYTL or MYTL. Full sequences of the primers and the constructs are available upon request. The CaMs with mutations in the $Ca^{2+}$ coordinating aspartate residues in the 1,2,3,4 and 2,3,4 EF hand domains were a gift from P. Adelman. They were subcloned into pcDNA-3 vectors for mammalian expression.
16. M. He, I. Bodi, G. Mikala, A. Schwartz, *J. Biol. Chem* **272**, 2629 (1997).
17. Neuronal transfection was done by a modified $Ca^{2+}$ phosphate method, as described (*36*). Neurons were transfected with a 2:1:1 ratio of α1C, β1b, and α2δ LTC subunits. For immunocytochemistry experiments, cells were cotransfected with a ratio of 6:1 channel subunits to green fluorescent protein (GFP). For luciferase assays, neurons were transfected with a ratio of 12:2:1 of channel subunits to CRE or MRE luciferase constructs and renilla luciferase driven by a thymidine kinase promoter as a transfection control. The CRE luciferase gene contains four copies of the somatostatin CRE upstream of firefly luciferase and is commercially available from Stratagene. The MRE luciferase construct contains three copies of the MRE upstream of firefly luciferase and was a gift of E. Olsen. Luciferase assays were performed 4 to 6 hours after stimulation with the Dual Luciferase Reporter assay system (Promega) and measured in duplicate on an automated luminometer (Lucy-2, Phoenix Research Products). Luciferase values are expressed either as raw ratios of firefly luciferase to renilla luciferase values (Figs. 4G and 5B) or as percent activation (Figs. 3C, 4A, and 5A) in which depolarization-induced activation of CRE-Luc or MRE-Luc in cells transfected with wild-type or mutant LTCs is normalized to the maximal reporter gene transcription in the transfected cells after depolarization in the absence of nimodipine. Transcription of the CRE-luciferase gene maximally increased 5- to 10-fold and the MRE luciferease gene 10- to 20-fold.
18. R. E. Westenbroek, L. Hoskins, W. A. Catterall, *J. Neurosci.* **18**, 6319 (1998).
19. Immunocytochemistry was performed with standard protocols. GFP-transfected cells were scored for pCREB $Ser^{133}$ or pERK $Thr^{202}/Tyr^{204}$ staining in a double-blinded fashion and in some cases analyzed with a cooled CCD camera to measure fluorescence intensity. A total of 1000 to 1200 cells were counted per condition. Values are given as the percentage of transfected cells (GFP-positive) that are also phospho-CREB– or phospho-Erk–positive.
20. A. Bonni, D. D. Ginty, H. Dudek, M. E. Greenberg, *Mol. Cell. Neurosci.* **6**, 168 (1995).
21. B. Z. Peterson, C. D. DeMaria, J. P. Adelman, D. T. Yue, *Neuron* **22**, 549 (1999).
22. R. D. Zuhlke, G. S. Pitt, K. Deisseroth, R. W. Tsien, H. Reuter, *Nature* **399**, 159 (1999).
23. A. Lee, *et al.*, *Nature* **399**, 155 (1999).
24. R. D. Zuhlke, G. S. Pitt, R. W. Tsien, H. Reuter, *J. Biol. Chem.* **275**, 21121 (2000).
25. B. Z. Peterson *et al.*, *Biophys. J.* **78**, 1906 (2000).
26. X. M. Xia *et al.*, *Nature* **395**, 503 (1998).
27. D. Chin, A. R. Means, *Trends Cell Biol.* **10**, 322 (2000).
28. Z. Mao, A. Bonni, F. Xia, M. Nadal-Vicens, M. E. Greenberg, *Science* **286**, 785 (1999).
29. F. S. Naya, E. Olson, *Curr. Opin. Cell Biol.* **11**, 683 (1999).
30. Y. Kato *et al.*, *EMBO J.* **16**, 7054 (1997).
31. J. Xing, D. D. Ginty, M. E. Greenberg, *Science* **273**, 959 (1996).
32. G. Y. Wu, K. Deisseroth, R. W. Tsien, *Proc. Natl. Acad. Sci. U.S.A.* **98**, 2808 (2001).
33. C. Cowan, M. E. Greenberg, unpublished data.
34. G. E. Hardingham, F. J. Arnold, H. Bading, *Nature Neurosci.* **4**, 261 (2001).
35. G. E. Hardingham, S. Chawla, C. M. Johnson, H. Bading, *Nature* **385**, 260 (1997).
36. R. E. Dolmetsch, M. E. Greenberg, unpublished data.
37. Z. Xia, H. Dudek, C. K. Miranti, M. E. Greenberg, *J. Neurosci.* **16**, 5425 (1996).


38. We thank T. Snutch, J. P. Adelman, and E. Olsen for LTC, CaM, and MRE luciferase constructs, respectively, E. Nigh for helpful discussions, and members of the Greenberg lab for critical reading of the manuscript. Supported by a NIH Mental Retardation Research Center grant (P30-HD18655) and grants from NIH (NS28829 to M.E.G.) and the McKnight Endowment for Neuroscience (to R.E.D. and M.E.G.). M.E.G. acknowledges the generous contribution of the F. M. Kirby foundation to the Division of Neuroscience. R.E.D is a Helen Hay Whitney Postdoctoral Fellow. J.M.S is an American Cancer Society Postdoctoral Fellow.

12 June 2001; accepted 8 August 2001


# Crystal Structure of the Extracellular Segment of Integrin αVβ3


**Jian-Ping Xiong,[1] Thilo Stehle,[1,2] Beate Diefenbach,[3] Rongguang Zhang,[4] Reinhardt Dunker,[3] David L. Scott,[1] Andrzej Joachimiak,[4] Simon L. Goodman,[3] M. Amin Arnaout[1]***



**Integrins are αβ heterodimeric receptors that mediate divalent cation-dependent cell-cell and cell-matrix adhesion through tightly regulated interactions with ligands. We have solved the crystal structure of the extracellular portion of integrin αVβ3 at 3.1 Å resolution. Its 12 domains assemble into an ovoid "head" and two "tails." In the crystal, αVβ3 is severely bent at a defined region in its tails, reflecting an unusual flexibility that may be linked to integrin regulation. The main intersubunit interface lies within the head, between a seven-bladed β-propeller from αV and an A domain from β3, and bears a striking resemblance to the Gα/Gβ interface in G proteins. A metal ion–dependent adhesion site (MIDAS) in the βA domain is positioned to participate in a ligand-binding interface formed of loops from the propeller and βA domains. MIDAS lies adjacent to a calcium-binding site with a potential regulatory function.**


Integrins are large heterodimeric cell surface receptors found in many animal species ranging from sponges to mammals [reviewed in (*1*)]. These receptors are involved in fundamental cellular processes such as attachment, migration, proliferation, differentiation, and survival. Integrins also contribute to the initiation and/or progression of many common diseases including neoplasia, tumor metastasis, immune dysfunction, ischemia-reperfu-